

Manipulation and adsorption-site mapping of single pentacene molecules on Cu(111)Jérôme Lagoute,¹ Kiyoshi Kanisawa,² and Stefan Fölsch^{1,*}¹*Paul-Drude-Institut für Festkörperelektronik, Hausvogteiplatz 5-7, D-10117 Berlin, Germany*²*NTT Basic Research Laboratories, NTT Corporation, Atsugi-shi, Kanagawa 243-0198, Japan*

(Received 10 June 2004; revised manuscript received 2 September 2004; published 10 December 2004)

Low-temperature scanning tunneling microscopy at 7 K is used to study the adsorption and manipulation of single pentacene molecules on Cu(111). Controlled lateral translations of the molecule are performed along different high-symmetry directions of the substrate via attractive tip-molecule interactions. By means of a detailed site-mapping technique combining lateral manipulations of the molecule and of native substrate adatoms we determine the adsorptive configuration of the aromatic molecule. We find a planar adsorption geometry with the long molecular axis aligned with the close-packed Cu atom rows and the benzene units centered over hexagonal close-packed hollow sites of the substrate.

DOI: 10.1103/PhysRevB.70.245415

PACS number(s): 68.43.Fg, 68.47.De, 82.37.Gk, 68.37.Ef

The interaction of organic molecules with solid surfaces is of central importance for various issues in science and technology. These include, for example, surface chemistry and catalysis,¹ basic steps during organic semiconductor layer growth,² and the concept of molecular electronics³ which aims at utilizing single molecules as functional building blocks with defined switching, sensing, or conduction properties. Especially with respect to the latter issue, low-temperature scanning tunneling microscopy (LT-STM) provides an excellent experimental approach since it allows to address, to characterize, and to manipulate^{4,5} single adsorbed atoms and molecules with atomic-scale precision. In this work, we employ LT-STM to explore the detailed adsorptive configuration of single pentacene molecules on the close-packed transition metal surface Cu(111). Pentacene (C₂₂H₁₄) is a linear polycyclic hydrocarbon and has recently gained ample attention due to its promising bulk properties as an organic semiconductor.⁶ By means of a detailed site-mapping technique which combines lateral manipulations of the molecule and of native substrate adatoms we perform a straightforward determination of the energetically preferred molecular adsorption site. It is demonstrated that LT-STM-based manipulation provides a powerful surface science tool which facilitates a direct real-space determination of the overall adsorption geometry of single organic molecules.

The experiments were performed with a homebuilt ultrahigh-vacuum (UHV) LT-STM system at a temperature of 7 K. A chemomechanically polished Cu(111) crystal was cleaned *in situ* by repeated Ne sputtering at 1 keV and annealing at 700 K. Molecules were deposited in UHV by thermal sublimation of pentacene after carefully degassing the crystalline source material. Cut Pt-Ir tips were used for the present experiments. Prior to the measurements the final tip condition was optimized by controlled tip-sample contact at 7 K. The metallic character of the tip was checked by spectroscopic measurements of the differential tunneling conductance dI/dV verifying inherent electronic features of the Cu(111) surface such as the onset of the surface-state band⁷ and a smooth variation of the local density of states within the pseudogap of the projected Cu bulk bands.⁸ Respective tunneling voltages indicated in the following refer to the sample bias with respect to the tip.

Figure 1(a) shows a constant-current STM image of an extended surface area (560 Å × 336 Å) after depositing $\sim 6 \times 10^{12}$ molecules per cm² at room temperature and subsequently cooling the specimen to the measuring temperature of 7 K. Single pentacene molecules appear as rodlike protrusions with lobes of enhanced tunneling conductance located at the ends. The wave pattern between the molecules arises from the Friedel oscillations of the Cu(111) surface-state electrons. As evident, no pronounced tendency of molecular clustering is observed which indicates the absence of appreciable attractive intermolecular interactions. This characteristic is advantageous for the present purpose, since it permits room-temperature sample preparation for experiments focused on single-molecule spectroscopy and manipulation. In contrast to the behavior found on homogeneous terraces, surface defects like steps act as effective sites for molecular aggregation. In detail, we find that quasiperiodic arrays of pentacene molecules with their long axis parallel to the step direction are formed preferably at the upper edge of monoatomic Cu steps. This specific behavior in heterogeneous nucleation, which was similarly observed for benzene molecules on Cu(111),⁹ is likely to arise from the interaction of adsorption-induced molecular dipoles^{10,11} with the intrinsic step dipoles present at a metal surface (the latter are due to the well known *Smoluchowski* effect of electron-charge smoothing¹²). At the same time, it indicates a considerable degree of surface diffusion of single pentacene molecules on Cu(111) at room temperature.

Turning back to the molecular adsorption on homogeneous terraces, a comparison between the STM image in (b) and the atomic corrugation of bare Cu(111) in (c) shows that the molecules strictly align with the close-packed Cu atom rows along the three equivalent $\langle 110 \rangle$ in-plane directions. The characteristic appearance of the molecule when imaged with a bare metallic tip is shown in Fig. 1(d). The diagram on the lower right details the corresponding constant-current profile measured along the long molecular symmetry axis at a tunneling current of 1 nA and a bias of 460 mV. The spacing of the observed double-lobe structure extracted from a large set of STM images is (9.8 ± 0.2) Å which is close to the separation of the outermost benzene rings of the free mol-

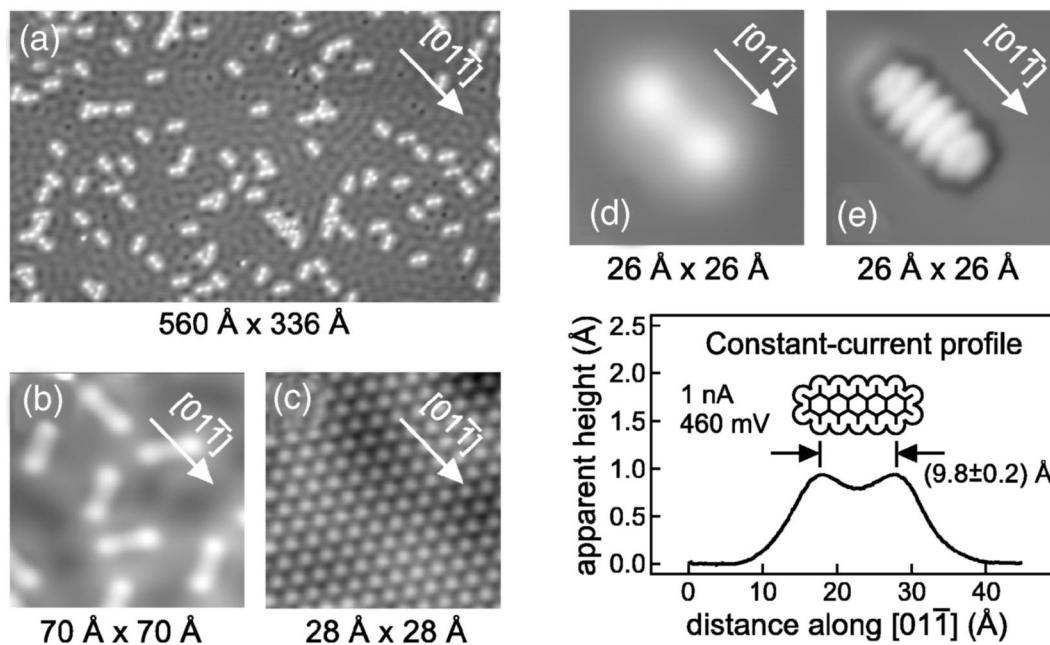


FIG. 1. Constant-current STM images of an extended Cu(111) surface area after depositing $\sim 6 \times 10^{12}$ pentacene molecules per cm^2 at room temperature and subsequently cooling to the measuring temperature of 7 K [(a), $560 \text{ \AA} \times 336 \text{ \AA}$, 1 nA, 5 mV] and of a smaller surface area [(b), $70 \text{ \AA} \times 70 \text{ \AA}$, 4.4 nA, 65 mV]; molecules are aligned with their long axis parallel to the close-packed Cu rows; cf. atomic corrugation of the bare surface in (c) [$28 \text{ \AA} \times 28 \text{ \AA}$, 0.1 μA , 65 mV]. Single molecules appear as rodlike features with an enhanced tunneling conductance at the ends; cf. (d) [$26 \text{ \AA} \times 26 \text{ \AA}$, 1 nA, 460 mV] and diagram on the lower right, whereas submolecular resolution is obtained when transferring a molecule to the tip prior to imaging an adsorbed molecule [(e), $26 \text{ \AA} \times 26 \text{ \AA}$, 5 nA, -100 mV].

ecule obtained in first-principles calculations.¹³ This signature in molecular imaging is present basically over the entire bias range investigated (from -2 V to 2 V). For negative bias voltages (i.e., in the regime of occupied states) the apparent molecular height is almost constant and amounts to $0.6\text{--}0.7 \text{ \AA}$, while for positive biases it continuously increases towards a value of $\sim 1.8 \text{ \AA}$ at 2 V . Contrasting the characteristic appearance as shown in Fig. 1(d), submolecular resolution is obtained when a single pentacene molecule is picked up by the tunneling tip prior to imaging an adsorbed molecule; cf. Fig. 1(e) (the conditions under which a molecule is transferred to the tip will be discussed below).¹⁴ In this case, a molecular corrugation is observed which is composed of five distinct lobes. Under these specific imaging conditions the overall molecular appearance resembles the spatial variation of the wave functions calculated for states of the isolated pentacene molecule close to the highest occupied and lowest unoccupied molecular orbital (HOMO-LUMO) gap.¹³ We interpret this finding as a clear indication that pentacene molecules adsorb in a planar geometry on Cu(111). This is a common feature of aromatic molecules adsorbed on metal surfaces.^{15,16}

To achieve a controlled lateral manipulation of single pentacene molecules, we systematically measured the tunneling current while performing line scans¹⁷ across the molecule at constant tip height and along different high-symmetry directions. Three cases are indicated in the top left panel of Fig. 2: namely, scanning parallel to the long molecular axis and the Cu rows along $[01\bar{1}]$ [labeled as (1)], scanning obliquely to the long axis and parallel to the Cu rows along $[10\bar{1}]$

[labeled as (2)], and scanning perpendicular to the long axis and parallel to the $[2\bar{1}\bar{1}]$ in-plane direction [labeled as (3)]. In each case, repetitive line scans were executed starting at an initial tip-surface separation of $\sim 6 \text{ \AA}$ while stepwise decreasing the tip height by 0.1 \AA with each scan. In this way, the critical threshold in tip height was determined at which a lateral manipulation of the molecule takes place. For each manipulation event discussed in the following, it was verified by subsequent imaging that the molecule was shifted by a pure lateral translation and remained intact during the procedure. The current profiles obtained for the static molecule prior to a manipulation event scale according to the fundamental relation for the tunneling current $I \sim \exp(-2\kappa z)$ with the decay constant κ and the tip height z . The open circles in diagram (1) in Fig. 2 show such a current profile obtained by scanning the tip from the starting position A to the final position B across the static molecule parallel to its long axis [case (1)]. Clearly, the current profile indicates an enhanced tunneling conductance at the molecular ends in accordance with the constant-current images in Fig. 1. To allow for a direct comparison, the current profile is rescaled to a tip height of $\sim 3.5 \text{ \AA}$ at which the threshold for lateral manipulation of the molecule towards point B is established. The current response during manipulation is shown by the solid line in diagram (1) and reflects the commensurate hopping of the molecule along the substrate surface corrugation.^{18,19} The detailed shape of this manipulation curve verifies that the molecule is trapped by the tip while it is manipulated across the surface: Starting the lateral tip displacement at point A the tip approaches the molecule and the increase in current follows the rescaled profile of the static molecule. Before the

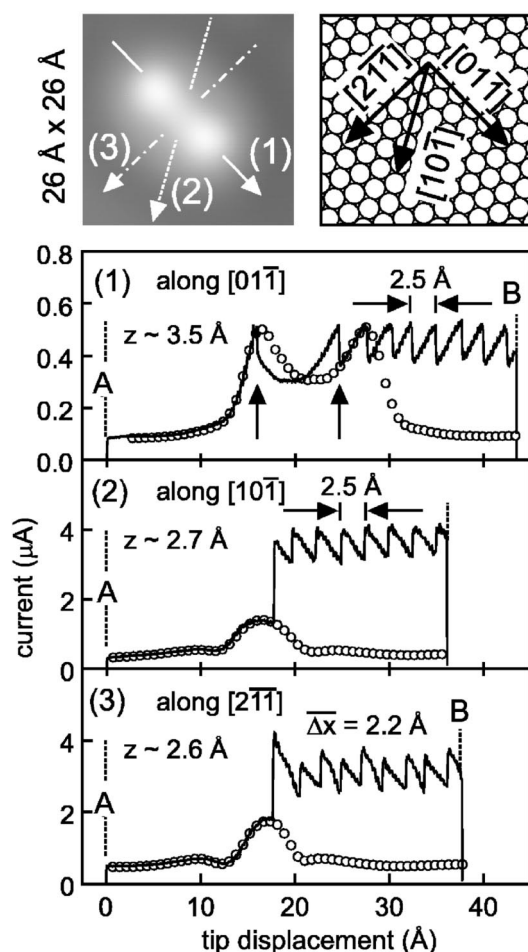


FIG. 2. Top panel: single-molecule STM image (left) and sphere model of the substrate (right) indicating three different directions labeled as (1), (2), and (3) along which lateral manipulation was performed (constant tip height, sample bias 300 mV). Bottom panel: diagrams showing the current response versus tip displacement (solid line) when manipulating the molecule along the directions (1), (2), and (3) by scanning the tip from A to B; open circles indicate rescaled current profiles measured for the static molecule prior to lateral manipulation. A tip scanning speed of 17 \AA/s was used throughout the manipulation experiment.

lateral tip position meets the molecular center, however, the molecule hops towards the tip to the left as indicated by a sudden drop in current marked by the left vertical arrow in diagram (1). This observation verifies an attractive interaction when approaching the molecule by the tip. After this initial jump, the characteristic current profile close to the molecular center is reproduced while the molecule eventually follows the tip by hopping back to the right; cf. current drop marked by the vertical arrow on the right. The subsequent current response during continued manipulation is composed of consecutive segments of the molecular profile resulting in a sawtoothlike signal which indicates that the overall interaction enforces a close proximity of the molecular center to the tip position. The period of the current modulation is $\sim 2.5 \text{ \AA}$, which is consistent with the interatomic spacing along the close-packed Cu rows ($a_0/\sqrt{2}=2.55 \text{ \AA}$, with the cubic Cu lattice constant $a_0=3.61 \text{ \AA}$). This suggests

that the molecule visits only one specific type of lattice site while it is manipulated along the Cu row direction of the surface.

The current response for manipulation according to case (2) (obliquely to the long axis and parallel to a Cu row direction) is shown in the center diagram of Fig. 2. Here, an increased proximity of the tip is required for a lateral translation of the molecule. The current response together with the rescaled molecular profile prior to manipulation (rescaled to a critical tip height of $\sim 2.7 \text{ \AA}$) clearly reflects that the molecule is manipulated via attractive interactions with the tip. In this case, however, a significant increase in current is observed during the manipulation and the response cannot be described solely by consecutive segments of the current profile of the adsorbed molecule. It is suggestive that this offset in current is due to a definite reorientation of the molecule within the tunneling gap (such as a partial “lifting”) which results in a reduced effective separation between the molecule and tip. This interpretation is supported by the fact that a further increase in proximity leads to less controllable translations frequently combined with molecular rotations or even with a transfer of the molecule to the tip. Similarly, a pronounced offset in current response is observed also for manipulation according to case (3) (perpendicular to the long axis and parallel to a $\langle 211 \rangle$ in-plane direction); cf. bottom diagram in Fig. 2. Here, the current response signal shows variations in the period and amplitude, indicating more complex changes of the molecular configuration within the tunneling gap. Yet the mean value of the period amounts to $\sim 2.2 \text{ \AA}$ which is in accordance with the close-packed Cu row spacing of $\sqrt{3/8}a_0=2.21 \text{ \AA}$ along the $\langle 211 \rangle$ in-plane direction.

We now address the observed trend in critical tip height at which the molecule is manipulated along the different high-symmetry directions. First, a certain degree of directional dependence in lateral manipulation may arise from the fact that the potential accounting for the tip-molecule interaction has to obey the symmetry requirements inherent to the adsorbed molecule. Second, the critical threshold for manipulation depends on the molecule-substrate interaction energy landscape experienced by the adsorbed molecule. This energy landscape will depend on the detailed bonding geometries and structural relaxations which are not available from the present data alone. Nonetheless, in order to interpret the observed behavior we propose a qualitative argument starting from the fact that an ideal incommensurate overlayer structure “floats” atop its substrate; i.e., the overlayer-substrate interaction energy is zero.²⁰ Bearing this general result in mind and assuming that the adsorbed pentacene molecule is not in perfect registry²¹ with the Cu(111) surface corrugation, it is suggestive that a smoother energy landscape variation would occur along the Cu row direction parallel to the long molecular axis [case (1)] than along a Cu row direction inclined to the long axis [case (2)]. This effect may be even enhanced by a different degree of nonregistry along the short- and long-symmetry axes of the molecule. In the hypothetical case of an infinitely extended and strictly periodic polyacene molecule which is incommensurate with the periodicity of the Cu rows, the energy landscape variation along the molecular axis would again vanish.

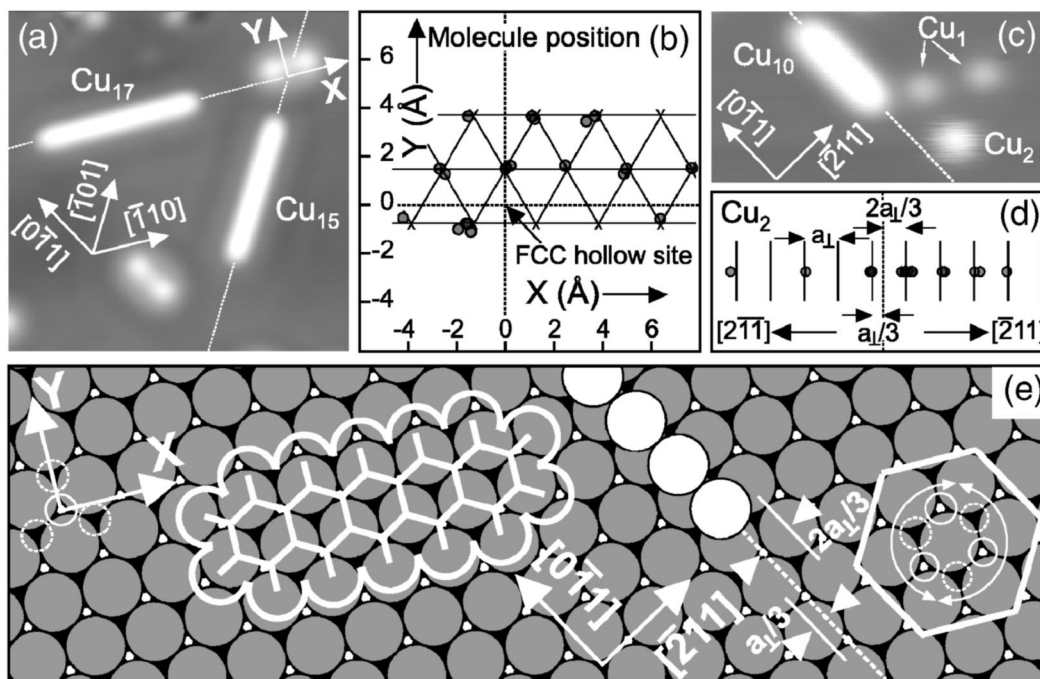


FIG. 3. (a) STM image ($105 \text{ \AA} \times 105 \text{ \AA}$, 1 nA, 500 mV) showing two assembled Cu adatom chains and a pentacene molecule located close to the intersection point of the chain directions (dashed lines). Diagram (b) summarizes positions of the molecular center with respect to the indicated coordinate system after repeated repositioning of the molecule (gray circles) and shows that only one specific lattice site is occupied. (c) STM image ($70 \text{ \AA} \times 35 \text{ \AA}$, 1 nA, 1V) of a Cu_{10} chain marking a reference line of fcc lattice sites (dashed line) together with a dimer (lower right) as a marker for an on-top site; values of the dimer-reference line separation measured after repeated dimer repositioning are drawn as gray circles in diagram (d). (e) Sphere model of the Cu(111) surface (gray: top layer, black: second layer, white: third layer) with a monatomic adatom chain (white spheres); the registry of the chain relative to the adjacent Cu rows of the substrate is also indicated. The hexagonal cell in which dimeric intracell diffusion occurs is shown on the right. The structure model of the planar pentacene molecule (bold white lines) indicates the adsorption geometry extracted from the site-mapping measurements with the molecular center located over a hcp hollow site of the substrate.

The manipulation data summarized in Fig. 2 were obtained at a sample bias of 300 mV while scanning the tip at constant height. On the basis of a large data set taken at various sample biases and tip heights it turns out that the specific result of a lateral manipulation procedure depends to a minor extent also on the tip condition such as the atomic-scale shape of the tip. Nevertheless, there is clear evidence for a general trend: We find only a moderate effect of the sample bias showing a slightly enhanced tendency towards molecular rotation and transfer to the tip for negative biases compared to positive biases. In contrast, the proximity of the tip represents the crucial parameter in determining whether the molecule is laterally shifted, rotated, or even picked up by the tunneling tip. This observation suggests that for the present system the tip-molecule interaction is governed primarily by attractive chemical forces rather than by effects of the tip-induced electric field.

Finally, the capability of controlled lateral manipulation is utilized to unambiguously determine the adsorption site of the single molecule. In a first step, Cu adatoms were created by controlled tip-surface contact at 7 K and monatomic Cu chains with the intrinsic Cu-Cu spacing of 2.55 \AA were assembled by atomic manipulation along the close-packed row direction.^{8,22} Apart from their intriguing electronic properties,⁸ these atomic-scale objects can be employed as markers for the surface lattice since the Cu chain atoms re-

side on face-centered-cubic (fcc) hollow sites of the substrate.²² The STM image in Fig. 3(a) shows a surface area where a Cu_{17} and a Cu_{15} chain were assembled by manipulating Cu adatoms along the $[\bar{1}10]$ and $[\bar{1}01]$ directions, respectively. The intersection point of the chain directions marks a fcc hollow site of the substrate. In the following, this reference point is chosen as the origin of a coordinate system with the x axis pointing along $[\bar{1}10]$ and the y axis pointing along $[\bar{1}\bar{1}2]$ [cf. upper right corner of Fig. 3(a)]. In a second step, a pentacene molecule was manipulated in the vicinity of the reference point including lateral translations and rotations of the molecule. The diagram in Fig. 3(b) summarizes the positions of the molecular center (cf. gray circles) relative to the fcc hollow site at $x=y=0$ extracted from a sequence of 19 manipulation events. Within a mean deviation of 5%, all measured positions lie on a (1×1) surface lattice as denoted by the hexagonal grid in the diagram (cf. solid lines). This shows that the center of the adsorbed molecule occupies only one specific lattice site. Within an accuracy of 8%, the three lattice points of the hexagonal grid closest to the origin are located at $[0, 2a_{\perp}/3]$ and $[\pm\sqrt{1/8}a_0, -a_{\perp}/3]$, respectively (here and in the following, the Cu row spacing $\sqrt{3}/8a_0$ along the $\langle 211 \rangle$ in-plane directions is abbreviated as a_{\perp}). Hence, the adsorption site under question corresponds

either to the on-top site or to the hexagonal-close-packed (hcp) hollow site of the substrate.

In order to distinguish between these two possibilities the crystallographic surface orientation has to be determined which again can be achieved by means of atomic manipulation. To do so, we applied a site-mapping technique similar to that introduced by Repp *et al.*²² In detail, we measured the distance between a monatomic Cu chain and a Cu dimer which was repetitively repositioned by manipulation. The STM image in Fig. 3(c) shows a Cu₁₀ chain assembled along $[0\bar{1}1]$ together with two Cu monomers and a Cu dimer to the lower right. As found by experiment and calculations,²² the Cu dimer diffuses locally at temperatures >5 K within a cell of adjacent hcp and fcc sites centered around an on-top site of the Cu(111) substrate. The corresponding hexagonal cell is depicted on the right of the sphere model in Fig. 3(e) together with the hcp sites (dashed lines) and the fcc sites (solid lines) centered around the on-top site. The intracell diffusion causes an unstable and round-shaped appearance of the Cu dimer in STM images^{8,22} as evident from the data in Fig. 3(c). In the present site-mapping procedure the Cu dimer serves as a marker for on-top site positions while the Cu chain determines a reference line of fcc sites along $[0\bar{1}1]$; cf. white dashed line in the STM image and in the sphere model. The diagram in Fig. 3(d) shows the measured positions of the Cu dimer (gray circles) with respect to the reference line (dashed vertical line) after repeated repositioning. The data are consistent with the spacing of $a_{\perp} = \sqrt{3/8}a_0$ between adjacent close-packed Cu rows as indicated by the vertical solid lines and yield the crystallographic orientation of the surface: The separation between the reference line and the nearest Cu row is $a_{\perp}/3$ along $[2\bar{1}\bar{1}]$ and $2a_{\perp}/3$ along $[\bar{2}11]$ as also illustrated in the sphere model. This information determines the relative arrangement of fcc and hcp sites at the substrate surface. Together with the molecular registry information [cf. Fig. 3(b)] it follows that the adsorbed molecule is centered over the hcp hollow site of the substrate. This adsorption geometry is illustrated in the sphere model where the structure of the planar molecule is indicated by bold white lines.

Owing to the fact that adsorption-induced molecular relaxations are common for benzene on close-packed transition metal surfaces,²³ it is likely that also pentacene adsorbed on Cu(111) adopts a relaxed conformation different from the structure of the free molecule. On the basis of the present experimental data alone, however, it is not possible to quantify structural intramolecular relaxations. Hence, for simplicity the dimensions of the free molecule¹³ were drawn in the

structure model in Fig. 3(e). Nonetheless, as a major characteristic of the adsorption geometry it is evident that respective benzene rings of the molecule are basically centered around hcp hollow sites. This observation is consistent with the overall behavior found by experiment^{23–25} and calculations^{26,27} for benzene adsorbed on various close-packed transition metals where the molecule occupies highly coordinated lattice sites (i.e., bridge sites and hollow sites) of the substrate. In the present case, however, a clear selectivity is found which favors the hcp hollow site over the fcc hollow site. A potential mechanism leading to an energetic non-equivalence between the hcp and fcc hollow sites may involve adsorption-induced relaxations not only of the molecule but also of the topmost substrate surface layers. Our present findings thus suggest that the substrate surface actively participates in the process of structural relaxation to lower the total energy of the system, rather than being a merely static template upon which adsorption occurs [it is noted that atomic-scale surface restructuring induced by adsorbed aromatic molecules has been reported recently for the Cu(110) surface²⁸]. We encourage future theoretical calculations to be combined with experimental structure data as provided here. Such a complementary approach will be most effective to address the difficult problem of bonding geometries and relaxation processes involved in the adsorption of organic molecules on surfaces.

In conclusion, the controlled lateral manipulation and adsorptive configuration of single pentacene molecules on the Cu(111) surface were investigated by LT-STM. Basic structural information on the adsorption geometry was extracted from a series of imaging and manipulation experiments. The planar molecule adopts a flat adsorption geometry with its long symmetry axis aligned with the close-packed Cu row directions along $\langle 110 \rangle$. The molecular center occupies exclusively the hcp hollow site of the substrate surface. LT-STM-based real-space information as obtained here is valuable since it provides direct insight into the adsorptive configuration of surface-supported organic molecules. The availability of this information is a prerequisite for studies of advanced complexity such as, e.g., the interaction and interconnection of single molecules with assembled atomic-scale surface structures.

The authors highly appreciate fruitful discussions with Jascha Repp and Gerhard Meyer. J.L. and S.F. gratefully acknowledge financial support by the European Union RTN Network Project NANOSPECTRA (Contract No. HPRN-CT-2002–00320).

*Corresponding author. Electronic mail: foelsch@pdi-berlin.de

¹N. D. Spencer and G. A. Somorjai, Rep. Prog. Phys. **46**, 1 (1983).

²F.-J. Meyer zu Heringdorf, M. C. Reuter, and R. M. Tromp, Nature (London) **412**, 517 (2001).

³C. Joachim, J. K. Gimzewski, and A. Aviram, Nature (London) **408**, 541 (2000).

⁴D. M. Eigler and E. K. Schweizer, Nature (London) **344**, 524

(1990).

⁵G. Meyer, S. Zöphel, and K. H. Rieder, Phys. Rev. Lett. **77**, 2113 (1996).

⁶See, e.g., X. L. Chen, A. J. Lovinger, Z. Bao, and J. Sapjeta, Chem. Mater. **13**, 1341 (2001).

⁷M. F. Crommie, C. P. Lutz, and D. M. Eigler, Nature (London) **363**, 524 (1993).

- ⁸S. Fölsch, P. Hylgaard, R. Koch, and K. H. Ploog, *Phys. Rev. Lett.* **92**, 056803 (2004).
- ⁹P. S. Weiss, M. M. Kamna, T. M. Graham, and S. J. Stranick, *Langmuir* **14**, 1284 (1998).
- ¹⁰P. G. Schroeder, C. B. France, J. B. Park, and B. A. Parkinson, *J. Appl. Phys.* **91**, 3010 (2002).
- ¹¹N. J. Watkins, L. Yan, and Y. Gao, *Appl. Phys. Lett.* **80**, 4384 (2002).
- ¹²R. Smoluchowski, *Phys. Rev.* **60**, 661 (1941).
- ¹³R. G. Endres, C. Y. Fong, L. H. Yang, G. Witte, and Ch. Wöll, *Comput. Mater. Sci.* **29**, 362 (2004).
- ¹⁴We note that the tip conditioning procedure leading to submolecular resolution as shown in Fig. 1(e) is reproducible and will be described in detail in a forthcoming publication.
- ¹⁵P. H. Lippel *et al.*, *Phys. Rev. Lett.* **62**, 171 (1989).
- ¹⁶V. M. Hallmark, S. Chiang, K.-P. Meinhardt, and K. Hafner, *Phys. Rev. Lett.* **70**, 3740 (1993).
- ¹⁷A tip scanning speed of 17 Å/s was used which is comparable to typical values previously reported for lateral manipulation experiments (cf., e.g., Ref. 19).
- ¹⁸L. Bartels, G. Meyer, and K. H. Rieder, *Phys. Rev. Lett.* **79**, 697 (1997).
- ¹⁹S.-W. Hla, K.-F. Braun, and K. H. Rieder, *Phys. Rev. B* **67**, 201402(R) (2003).
- ²⁰A. Zangwill, *Physics at Surfaces* (Cambridge University Press, Cambridge, England, 1988).
- ²¹The spacing of benzene units of the free molecule is 2.45 Å (cf. Ref. 13) whereas the Cu-Cu spacing along $\langle 110 \rangle$ is 2.55 Å. Note, however, that the dimensions of the free molecule can at best serve as a rough estimate when compared to the adsorbed molecule.
- ²²J. Repp, G. Meyer, K. H. Rieder, and P. Hylgaard, *Phys. Rev. Lett.* **91**, 206102 (2003).
- ²³R. F. Lin, G. S. Blackman, M. A. Van Hove, and G. A. Somorjai, *Acta Crystallogr., Sect. B: Struct. Sci.* **43**, 368 (1987).
- ²⁴P. S. Weiss and D. M. Eigler, *Phys. Rev. Lett.* **71**, 3139 (1993).
- ²⁵G. Held, *Appl. Phys. A: Mater. Sci. Process.* **76**, 689 (2003).
- ²⁶P. Sautet and M.-L. Bocquet, *Phys. Rev. B* **53**, 4910 (1996).
- ²⁷J. R. Lomas and G. Pacchioni, *Surf. Sci.* **365**, 297 (1996).
- ²⁸M. Schunack, L. Petersen, A. Kühnle, E. Lægsgaard, I. Stensgaard, I. Johannsen, and F. Besenbacher, *Phys. Rev. Lett.* **86**, 456 (2001).